DOI: 10.1002/cphc.200800455

Molecular Mechanisms Causing Anomalously High Thermal Expansion of Nanoconfined Water

Stephen H. Garofalini,*[a] Thiruvilla S. Mahadevan,[a] Shuangyan Xu,[b] and George W. Scherer[b]

Anomalously high thermal expansion is measured in water confined in nanoscale pores in amorphous silica and the molecular mechanisms are identified by molecular dynamics (MD) simulations using an accurate dissociative water potential. The experimentally measured coefficient of thermal expansion (CTE) of nanoconfined water increases as pore dimension decreases. The simulations match this behavior for water confined in 30 Å and 70 Å pores in silica. The cause of the high expansion is associated with the structure and increased CTE of a region of water ~6 Å thick adjacent to the silica. The structure of water in the first 3 Å of this interface is templated by the atomically rough silica surface, while the water in the second 3 Å just beyond the atomically rough silica surface sits in an asymmetric potential well and displays a high density, with a structure comparable to bulk water at higher pressure.

1. Introduction

The behavior of nanoconfined water has been studied in recent years because of its importance in geomorphology, architectural stones, desalination membranes, and biological membranes where water is confined by hydrophilic or hydrophobic surfaces. The work presented here is related to the former.

Early work by Derjaguin et al.[1] showed anomalous expansion of water confined within 50 Å pores in silica xerogels. They determined that the difference in the structure of confined water and bulk water disappeared at 70 °C. More recent experiments shown here and elsewhere[2] indicate that the difference in coefficient of thermal expansion (CTE) increases with decreasing pore size and the CTE of water confined in 30 Å pores in silica equals that of bulk water at a temperature ~16 °C higher. The latter experiments provide precise data for the change in volume with temperature for water confined within nanopores that constitute a rigorous standard to which computational studies could be compared.

The structure of water confined in Vycor, a porous silica glass containing 40–80 Å pores, has been studied using both experimental and computational techniques.[3–11] Neutron diffraction experiments indicate a change in the structure of the confined water, and structural changes are observed in MD simulations.[5,10] However, there are contradictory results. In one case the results are interpreted to mean that water in the center of the pores has a structure similar to bulk water at a temperature 30 °C higher,[9] but another study concludes that water in the pore interior is similar to bulk water,[7] both of which contradict other data that indicates the water confined in 150 Å pores is similar to bulk water at a temperature 15 K lower.[12] Similarly, water within 5 Å of the interface is believed to have a change in bonding and structure that is said to lead to less bonding[5,7] or to more bonding.[12]

Density profiles of water as a function of distance from the pore center to the silica surface show a 5 Å thick layer with elevated density in simulations.[4,5] These, and other simulations of water/silica interfaces (where in some cases the silica is modeled as a quartz surface rather than glassy silica) all show a significant increase in the density of water at the interface. The peaks in density range from 20% above bulk water density[4,5,9,13] to 50%,[14,15] and even higher.[16,17]

In all of the previous simulations of confined water in silica, the water is modeled as rigid or flexible molecules using SPC, SPC/E, or TIP4P potentials and, in most cases, frozen silica. The silica surfaces are manually hydroxylated to create the surface silanols expected on real surfaces. All such simulations ignore the important dissociative chemisorption of water on silica, the rupture of strained siloxane bonds by water, the possible penetration of water and silanol formation into the sub-surface via openings in the ring-like network structure of silica, and the relaxation of the atoms in the silica while interacting with water molecules. Most importantly, none of these popular water potentials reproduce the liquid equation of state to the level needed to evaluate the anomalous expansion of confined water for comparison to experiment.

To achieve a more realistic simulation of the behavior of water confined in silica nanopores, we employed a newly developed dissociative water potential that matches many bulk water properties, such as the structure, heat of vaporization

[a] *Prof. S. H. Garofalini, Dr. T. S. Mahadevan*
Department of Materials Science and Engineering
Rutgers University, Piscataway, NJ (USA)
Fax: (+1) 732 445 3258
E-mail: shg@rutgers.edu

[b] *Dr. S. Xu, Prof. G. W. Scherer*
Department of Civil and Environmental Engineering
Princeton University, Princeton, NJ (USA)

(MD = 10.5 kcal mol^{-1} vs EXP = 10.52 kcal mol^{-1}), diffusion coefficient (MD = 2.45 cm^2 s^{-1} vs EXP = 2.3 cm^2 s^{-1}), dipole moment (MD = 2.6D vs exp = 2.6D), liquid–vapor coexistence curve, and the liquid equation of state.[18] This potential has been used to study the interactions between a silica-glass surface and water.[19] Results showed dissociative chemisorption of the water, silanol concentration consistent with experiment, and reaction mechanisms that included the formation of hydronium ions at the interface[19] that are completely consistent with ab-initio MD simulations.[20] Details of the generation of the potentials and cross-interactions were previously presented.[18,19] The new dissociative water potential offers the unique ability to reproduce the interactions occurring at the confined water/silica interface, allowing realistic simulation of the change in volume, *V*, as a function of temperature, *T*.

2. Results and Discussion

2.1. Volume–Temperature Behavior

MD simulations using plates of amorphous silica separated by 30 and 70 Å films of water are performed at several temperatures to evaluate expansion behavior. The water reacted with the silica surfaces, as in previous studies of water adsorption and reactions on silica surfaces using this dissociative water potential.[19] Results of the simulations are shown in Figure 1,

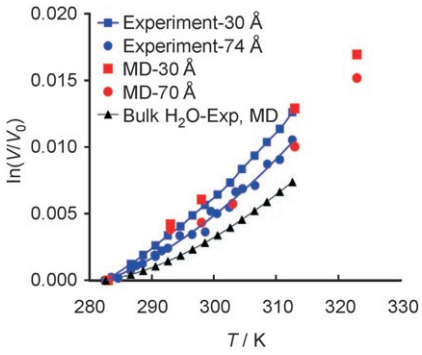

Figure 1. Normalized volume change with temperature for two pore sizes and bulk water for experimental data and molecular dynamics (MD) simulations.

along with experimental data for bulk water and water confined in silica xerogels with 30 and 70 Å pores. The simulations were previously shown to match *V*(*T*) of bulk water.[18] In Figure 1, the simulations show the changes in *V*(*T*) for confined water consistent with the experimental results for both pore sizes. The experiments clearly show that confinement causes an increase in CTE in comparison to bulk water, but shed no light on the atomistic mechanisms responsible for this behavior. However, since the MD simulations reproduce the experimental trends, it is reasonable to use them to investigate the mechanisms. Results involving the structure of the simulated systems are presented below primarily for the 30 Å film, although the results for interfacial and interior structure apply to both thicknesses.

2.2. Density Distribution and Structure of Nanoconfined Water

The density of atoms as a function of distance perpendicular to the interfaces for the 30 Å film at 298 K is shown in Figure 2. The results show three major features that differ from

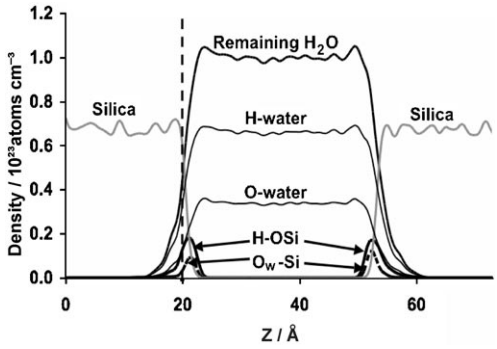

Figure 2. Density profiles of species as a function of distance perpendicular to the interfaces. Silica = original Si and O in silica, Remaining H_2O = water molecules remaining after reactions with glass, O–water = oxygen in remaining water molecules, H–water = hydrogen in remaining water molecules, O_w–Si = oxygen originally in water that chemisorbed and bonded to Si, H–OSi = hydrogen attached to any O that is bonded to Si. The latter two species indicate silanols.

all previous studies of confined water in silica. First, there is only a small (~5%) increase in density of water at the interface; in contrast, all other simulations that used the popular rigid water potentials show increases in water densities $\geq$20%. Second, water molecules react with the silica surface, forming silanols. These dissociatively chemisorbed water molecules are shown in Figure 2 as the distribution of oxygen from the water that is attached to a silicon (labeled O_w–Si) and hydrogen, attached to any oxygen, that is attached to a silicon (H on silanols and labeled H–OSi). Third, undissociated water molecules migrate into the glass via openings in the normal ring structure of silica. The reactions and penetration of water extend about 7 Å below the outermost surface oxygen.

In one case, it has been inferred that the water in the interior of nanopores in silica has a structure consistent with bulk water 30 °C warmer.[9] To evaluate the structure of our confined water, O–O pair distribution functions (OO–PDFs) of oxygen in water are generated as a function of location parallel to the water/glass interface for the 30 Å water system. The results from the 70 Å system are very similar. While all data below will involve the interface at the lower *Z* dimension, results are similar for the interface at the upper *Z* dimension. Starting from the *Z* = 20 Å location on Figure 2 (vertical dashed line), 2D OO–PDFs were generated for water molecules located within volume elements 3 Å thick (in *Z*) parallel to the interface for the 30 Å film. Results are shown in Figure 3 a, along with similar data for bulk water. The curve from 35 Å–38 Å is indicative of the structure of water in the interior of the pore (away from the water/silica interface); it is lost behind the bulk water curve, indicating that the water in the interior of the pore is very similar to bulk water. Other locations in the interior of the

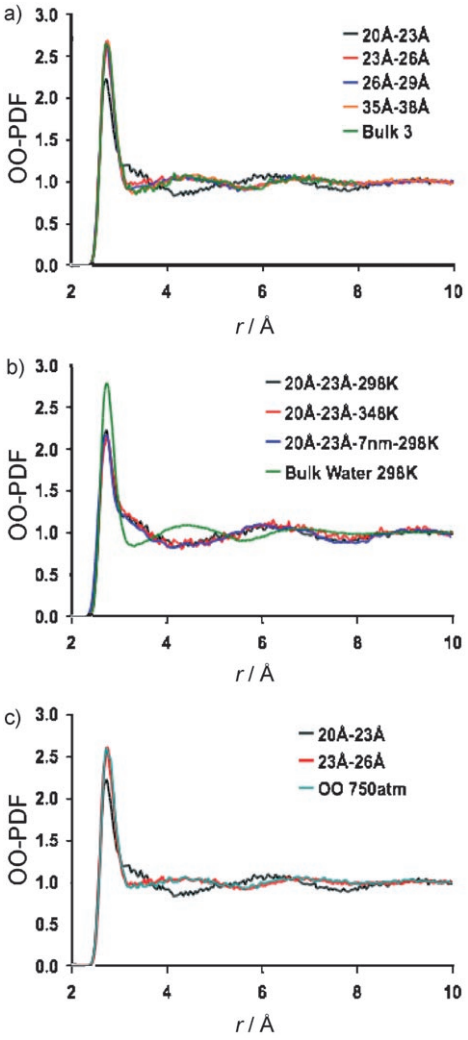

Figure 3. a) OO pair distribution function (PDF) for 3 Å regions as a function of distance starting from the interface at 20 Å in Figure 2, plus bulk water using a summation of 3 Å regions over the entire bulk. b) OO PDF for oxygen in physisorbed water on the silica surface at two temperatures for the 30 Å film, showing little change in structure with temperature, and in the 70 Å film, showing little change with film thickness. c) OO PDF for oxygen in the 30 Å film for the two layers of water closest to the interface and that for OO in bulk water at 750atm, showing the similarity between water at higher pressure and the water in the high density region near the interface (cf. Figure 2).

pore give similar results. This is similar to some studies,[7] but quite different from another[11] that shows a change in the water structure extending from the water/silica interface to the center of a 40 Å pore.

The structure of a glassy silica surface is shown in Figure 4, which is a snapshot of the top of a simulated glass surface in which the size of the O ions in the drawing is exaggerated to emphasize the rugosity of the structure. This atomically rough surface allows for physisorbed water molecules to be coincident with outer O from the glass surface, as seen in the density distributions in Figure 2 at the interfaces. The 20–23 Å OO–PDF curve, using only oxygen from water molecules, is generated from water physisorbed on the atomically rough silica surface and clearly shows the greatest change in structure

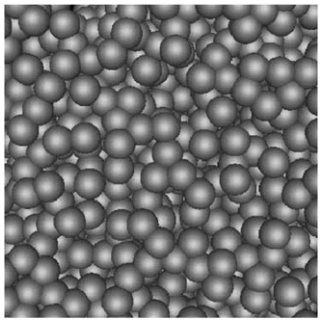

Figure 4. Snapshot of a silica glass surface with the size of the oxygen exaggerated to emphasize the atomistic roughness of the surface.

from that of bulk water. Owing to the templating effect of the very stable silica surface, this structure shows little change with temperature, as shown in Figure 3b with the OO–PDF from water in the 20–23 Å range at 298 K and 348 K. The structure of this region at 298 K is the same in the 30 and 70 Å films, showing that the pore dimension did not affect this interface structure.

The structure of water farther from the interface (23–26 Å and 26–29 Å) shows smaller deviations from bulk water as the distance from the interface increases, as shown in Figure 3a. Water beyond ~7–10 Å from the interface has a structure similar to bulk water. Therefore, the behavior causing the anomalously high CTE of confined water is located near the interface. This accounts for the data in Figure 1: the smaller the pore, the greater the ratio of the affected interfacial volume to total pore volume, resulting in a greater influence of the interface on the properties of the pore.

The water just beyond the end of the silica surface, at 23–26 Å, is clearly different from bulk water at the first minimum (~3.4–3.5 Å). This increase in the intensity of the OO–PDF at the first minimum has been observed for water at elevated temperature as well as water at higher pressure. However, higher temperature water shows a decrease in the intensity of the first maximum and a broadening of that peak that are incompatible with the 23–26 Å curve. The density profile in Figure 2 shows a 5% higher density in the 23–26 Å region than bulk water, which, on average, is similar to water at a pressure near 750 atm. Figure 3c shows that the OO–PDF for simulated bulk water at 750 atm (75 MPa) and 298 K is very similar to that for the 23–26 Å region, indicating that the structure near the interface is similar to that of bulk water at higher pressure. The effect of pressure on structure has been previously discussed.[21] However, the similarity to high pressure water is limited.

2.3. Cause of High Expansion in Nanoconfined Water

The simulations of nanoconfined water were done at 1 atm, not at elevated pressure, so the cause for the density increase near the interface is the interactions with the glass surface, resulting in an energy minimum in the 23 Å location. Figure 5 shows the average energy per atom as a function of distance perpendicular to the interface from the interface (20 Å) into

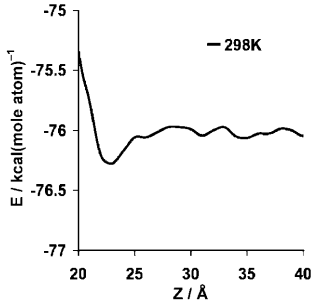

Figure 5. Average energy per atom in water molecules as a function of distance perpendicular to the interface (see Figure 2) showing the potential well near 23 Å that attracts water, creating the high density region, and the asymmetry in the energy curve adjacent to the well.

the interior of the confined water (40 Å), showing an energy minimum near 23–24 Å. This creates an attractive force to this location, resulting in the higher density. The enhancement in binding energy between this high-density region and the interior of the confined water film is ~1 kcal mole^{-1} of water molecules. The curve in Figure 5 also indicates an asymmetry in forces, with a higher repulsive wall in the $-Z$ direction and a lower barrier in the $+Z$ direction.

The number of hydrogen bonds per oxygen in the different volume regions and bulk water is shown in Figure 6. A H-bond

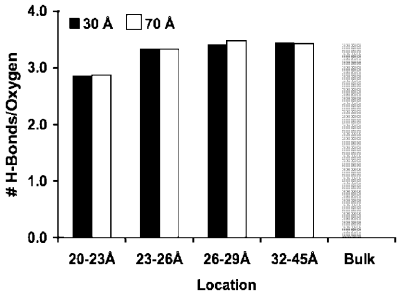

Figure 6. Number of hydrogen bonds per oxygen in water molecules as a function of region perpendicular to the interface and for bulk water.

is defined as having an O–H distance less than 2.4 Å and an H–O–O angle less than 30°. H-bonds at the interface include silanols as H-bond donors or acceptors interacting with O in water at the interface (H-bonds from silanols to any O bonded to Si are not included). The number of hydrogen bonds per oxygen in the interior of both the 30 Å and 70 Å films is similar to that of bulk water, with a slight decrease in the 23–26 Å region (which is consistent with water under higher pressure) and a greater decrease at 20–23 Å due to the presence of the silica.

The structure that we observe in these simulations with the dissociative water potential shows results consistent with the anomalous expansion of confined water that is observed experimentally. This structure deviates from what has been observed in simulations using non-dissociative (rigid or flexible) water potentials. The structure in the higher density region (23–26 Å) is consistent with water at high pressure, based on the OO–PDF. It is known that water at high pressure shows higher thermal expansion than normal bulk water,[22] so the enhanced CTE shown in Figure 1 can be attributed to this high density region. The change in density as temperature is increased in the confined water shows that the interior region (35–38 Å, and even thicker interior regions) behaves similarly to bulk water; however, the density of water near the interface (23–26 Å) decreases faster than bulk water (again, consistent with the effect of high pressure on expansion). In fact, both the 20–23 Å layer and the 23–26 Å layer decrease in density more rapidly than bulk water. Using ρ^* as the ratio of the density of the layer normalized by the bulk water density at that temperature, a plot of $\ln(\rho^*)$ vs T is linear, indicating that the relative density change of a layer to that of the bulk is constant over this T range. The slope of this plot results in a CTE of the combined layers from 20–26 Å equal to 5.9 e^{-4}°C^{-1}. Using this 6 Å layer as the relevant high expansion region, times 2 for both interfaces, means that the interface contributes 40% to the volume of the 30 Å film and 17% to the 70 Å film. A calculation of the contribution to CTE of the confined film from the interfacial layer plus the interior (which has the bulk water CTE) indicates that the interfacial region must have a CTE near 6.4 e^{-4}°C^{-1} for the 30 Å film and 6.7 e^{-4}°C^{-1} for the 70 Å film to account for the CTE of the confined films. These results are very close to the 5.9 e^{-4}°C^{-1} value obtained in the interface in the simulations. Thus, the simulations show that the higher CTE of the 6 Å of water at the interface creates the observed higher CTE of the confined water. The volume fraction of the interface in a spherical or cylindrical pore is larger than in a film, but the experimental systems had a range of pore sizes (albeit narrow), so more precise comparisons are not meaningful.

In contrast to hydrostatically compressed water, the interfacial layer is in a highly asymmetrical potential well (Figure 5), where movement toward the glass surface is energetically blocked. Consequently, thermal agitation tends to drive water molecules from the interface toward the interior of the pore, leading to a net larger volume expansion.

3. Conclusions

We conclude that the anomalously high CTE of nanoconfined water results from the high expansion of the ~6 Å layer at the surface of the pore caused by the local density and asymmetry of the potential well. Simulation of this behavior of nanoconfined water requires an interatomic potential that accurately reproduces the liquid equation of state for bulk water and allows for an accurate representation of the reactions and interactions between water molecules and the silica surface. The density and strength of binding of this layer can be accurately described using the recently developed dissociative potential for water, enabling simulation results similar to the experimental data for the expansion of nanoconfined water. The dissociative potential gives results that are quantitatively, and in some cases qualitatively, different from previous simulations based on rigid water molecules.

Methodology

The experimental method has been described in ref. [2]. The molecular dynamics simulations used an amorphous silica made via a melt-quench process similar to that published in ref. [19]. In the current case, the silica glass dimensions are ~64 Å x 64 Å x 40 Å in *X*, *Y*, and *Z*, with the water film filling *X* and *Y* and ~30 Å thick or ~70 Å thick in *Z*, with periodic boundaries in all directions. The simulations were done in modified NPT (constant number, pressure, temperature) conditions, with constant *X* and *Y* dimensions and a constant pressure of 1 atm applied in the *Z* dimension, allowing the system to expand or contract as a function of temperature in the *Z* direction. Simulations of 1 000 000 moves per temperature were run with a timestep of 1 e^{-16} s, with volume becoming stabilized within the first 200 000 moves. The volume was averaged over the last 40% of each run. Simulations of bulk silica alone at each temperature were used to generate the *V*(T) data for silica, which was subsequently subtracted from the total volume of the combined water/silica system in order to generate the volume change of the water.

Acknowledgements

The authors wish to acknowledge funding from the DOE Office of Science, Division of Material Sciences, grant number, DE-FG02-97ER45642.

Keywords: glass · interfaces · molecular dynamics · nanomaterials · water

[1] B. V. Derjaguin, V. V. Karasev, E. N. Khromova, *J. Colloid Interface Sci.* **1986**, *109*, 586–587.
[2] S. Xu, G. C. Simmons, G. W. Scherer, *Mater. Res. Soc. Symp. Proc.* **2004**, *790*, 85–91.
[3] P. Gallo, M. Rovere, M. A. Ricci, C. Hartnig, E. Spohr, *Phil. Mag. A* **1999**, *79*, 1923–1930.
[4] E. Spohr, C. Hartnig, *J. Mol. Liq.* **1999**, *80*, 165–178.
[5] M. A. Ricci, F. Bruni, P. Gallo, M. Rovere, A. K. Soper, *J. Phys. Condens. Matter* **2000**, *12*, A345–A350.
[6] P. Gallo, M. Rovere, M. A. Ricci, C. Hartnig, E. Spohr, *Europhys. Lett.* **2000**, *49*, 183–188.
[7] C. Hartnig, W. Witschel, E. Spohr, P. Gallo, M. A. Ricci, M. Rovere, *J. Mol. Liq.* **2000**, *85*, 127–137.
[8] M.-C. Bellissant-Funel, *J. Phys. Condens. Matter* **2001**, *13*, 9165–9177.
[9] P. Gallo, M. A. Ricci, M. Rovere, *J. Chem. Phys.* **2002**, *116*, 342–346.
[10] V. Crupi, D. Majolino, P. Migliardo, V. Venuti, M. C. Bellissent-Funel, *Mol. Phys.* **2003**, *101*, 3323–3333.
[11] H. Thompson, A. K. Soper, M. A. Ricci, F. Bruni, N. T. Skipper, *J. Phys. Chem. B* **2007**, *111*, 5610–5620.
[12] J. Dore, *Chem. Phys.* **2000**, *258*, 327–347.
[13] A. A. Hassanali, S. J. Singer, *J. Phys. Chem. B* **2007**, *111*, 11181–11193.
[14] N. Giovambattista, P. J. Rossky, P. G. Debenedetti, *Phys. Rev. E* **2006**, *73*, 041604.
[15] S. H. Lee, P. J. Rossky, *J. Chem. Phys.* **1994**, *100*, 3334–3345.
[16] T.-D. Li, J. Gao, R. Szoszkiewciz, U. Landman, E. Riedo, *Phys. Rev. B* **2007**, 75.
[17] E. J. W. Wensink, A. C. Hoffman, M. E. F. Apol, H. J. C. Berendsen, *Langmuir* **2000**, *16*, 7392–7400.
[18] T. S. Mahadevan, S. H. Garofalini, *J. Phys. Chem. B* **2007**, *111*, 8919–8927.
[19] T. S. Mahadevan, S. H. Garofalini, *J. Phys. Chem. C* **2008**, *112*, 1507–1515.
[20] Y. Ma, A. S. Foster, R. M. Nieminen, *J. Chem. Phys.* **2005**, *122*, 144709.
[21] A. G. Kalinichev, Y. E. Gorbaty, A. V. Okhulkov, *J. Mol. Liq.* **1999**, *82*, 57–72.
[22] L. T. Minassian, P. Pruzan, A. Soulard, *J. Chem. Phys.* **1981**, *75*, 3064–3072.

Received: July 21, 2008
Published online on September 11, 2008

